**Journal of Engg. Research EMSME Special Issue pp. 133-145** DOI : 10.36909/jer.EMSME.13899

# Optimization of Process Parameters of Pin on Disc Wear Set up for 3D Printed Specimens

Harish Kumar*, Anuj Sharma**, Yogesh Shrivastava***, Shahroz Akhtar Khan*** and Pawan Kumar Arora***

**Department of Mechanical Engineering, National Institute of Technology Delhi,India*
***Centre for Advanced Studies, Dr. A P J Abdul Kalam Technical University (CAS-AKTU), Lucknow, India*
****Department of Mechanical Engineering, Galgotias College of Engineering and Technology, Gautam Budh Nagar, India*
*Corresponding Author: pawan.arora.1976@gmail.com*

## ABSTRACT

3D Printing is av  technology that produces three-dimensional parts layer by layer from a material. The method relies on a digital data file being transmitted to a machine that then builds the component. The evolution of 3D printing has seen rapid growth in the manufacturing industry. However, the material properties of the fabricated part are different for different combinations of input parameters. Hence, it is essential to determine the properties of the fabricated specimen.  In the present work, specimens of ABS have been fabricated using a 3D printer conform to ASTM G99 standard, by varying the combinations of input parameters. The design of experiments has been done using Box Behnken design. Thereafter, the wear rate of the fabricated specimens has been tested on the wear tester machine (Pin-on-disc). The obtained combination of input and output has been used to generate a mathematical model using response surface methodology (RSM). The model has been optimized and a suitable range of input parameters have been determined, pertaining to the minimum wear rate for given conditions.

**Keywords:** Additive manufacturing; Pin on disc; Full factorial design; Fused filament fabrication.

## INTRODUCTION

In recent years, additive manufacturing (AM) technology has progressed significantly. With tailored material properties and ease to create intricate geometries. AM technology has gained a tremendous industrial and academic curiosity all through its development (Calignano et al.,2017). Manufacturing industries have witnessed an overall reduction of time in the process of product design and manufacturing with adapt to AM technology. AM technology with ease in withstanding flexible and dynamic design changes stand out as a solution to iron out chaos into product design sequences. The AM technology offers vast solutions to the issues faced by manufacturing industries. Although these industries may have distinct objectives for implementing AM technologies to their core processes, one can opt from a variety of AM processes available for promising scalable manufacturing solutions and allowing to accommodate future changes in the production line. Emerged as the most promising way to manufacture items, AM technology is currently been used in industries with growing numbers (Negi et al., 2014). In the recent past, AM technologies have marked a significant presence in almost every sector whether it be the medical, automobile,-consumer products, or aviation with the applications allowing to produce a functional-prototype to the final assembly models.

Conventional product manufacturing technology involves material removal from raw material to shape it up into desired product. However, it is a broadly acknowledged and utilized way to fabricate any item, it faces challenges in facilitating dynamic design changes and in producing an intricately shaped item. Contrary to conventional manufacturing, AM is a method to produce an item by adding material layer-over-layer in a predefined way. A complete additive process involving the creation of CAD model to the final product involves making use of a computer, CAD software, an AM machine, and a layering material. Here the advantage lies in creating a 3D model of the part to be produced (or printed) first on a computer with the help of a computer-aided design (CAD) software and when any corrections or modifications are required in the final design, the CAD model is updated with the same before fabrication. AM techniques are now been developed for product fabrication with a large choice of materials belonging to low-grade resins, polymers, metals, metal-composites, alloys, and ceramics in close-loop control applications (Srivastava et al., 2018, Yadav et al., 2021 & Mercado et al., 2020).

The CAD file so created with information of 3D model for the item to be produced is then converted to Standard Tessellation Language (.STL) file which saves the CAD model into a wire-mesh form. When AM machine is fed with the STL file it read the data and converts it to 2D slicing (layering) information for the same 3D model. The popular CAD software that can solve the task completely, from creating a 3D model for the item to be fabricated to converting or saving the same to STL file format, are Autodesk Inventor, Solid Works, Fusion 360, etc. The preprocessing software on the machine embeds with each layer the instruction for the tool-path before printing.

Polymers with good formability characteristics in liquid, solid, and powdered forms are employed as the layering material. The early idea of AM developed around 1980 utilizing the photosensitive resin that gets transformed into a solid form with UV light progressively falling on it (Gao et al., 2015). The interaction of photosensitive resin with UV light results in creating a layer of the part to be produced in succession one over the other, justifying the word 'additive' associated with this process (Mellor et al., 2014 & Selimis et al., 2017). The American Society for Testing and Materials (ASTM) in the year 2010 set up standards to lay out seven categories of AM processes and clubbed them under jurisdiction of subcommittee ASTM F42.05. Vat Polymerization, material jetting, binder jetting, fused deposition modeling (FDM), powder bed fusion, sheet lamination, and directed energy deposition form basic recognized categories as per ASTM F42.05 alongwith basic standard terminology recognition under a subcommittee ASTM F42.91 (ASTM International, 2012, ISO/ASTM52900-15, 2014 & Gibson et al., 2014).

FDM technique, for being economical and employing an uncomplicated setup, is the most common to fabricate the product additively. This technique utilizes polymers in the form of the wired filament. During preprocessing, when the FDM machine is fed with an STL file with CAD data, process parameters and work-orientation need to set to broken down the 3D mesh model into slices or layers embedded with tool-path instruction. Reading this layer-wise information, the FDM machine, usually called a 3D printer, draws a wired filament of polymer from the spool into a heated-head with a nozzle where it melts down and gets extruded onto a build-platform. FDM technique has its noticeable presence in prototyping (Novakova, 2012), bone-implant (Sahmani et al., 2020 & Agnieszka et al., 2020), customize oral drug-delivery (Sylvain et al., 2021, Alhijjaj et al., 2016, Yang et al., 2018 & Kejing et al., 2021), biomedical (Chohan et al., 2017, Ahangar et al., 2019 & Plocher et al., 2019), and aerospace (Kumar et al., 2017 & Chandrasekar et al., 2021) industry to keep coping with the changing customer demands.

Acrylonitrile Butadiene Styrene (ABS), Poly Lactic Acid (PLA), and Nylon are the polymers popularly used in the FDM process and are available commercially in the form of wired-filament (Tiwary et al., 2015 & Makara et al., 2019). Selection between the polymers can easily be made based on mechanical properties (as shown in Table 1) they exhibit along with other factors which, in some cases, affect the selection to a large. Visual quality is one such factor that measures the appearance of the fabricated part. Ease of printing is another important criterion affecting one's decision during polymer selection. It is a significant criterion measured over the variability of conditions like bed-adhesion, speed range for printing, flow accuracy and ease to feed into the 3D printer, etc. The selection should meet the objective of fabricating high-quality parts at a low cost and time to meet the growing market need (Makara et al., 2019 & Patel et al., 2012).

**Table 1.** Relative comparison of the polymers popularly used in FDM process

| | Criteria | | | | | | |
|---|---|---|---|---|---|---|---|
| **Poly-mers** | **Maximum Stress** | **Impact Resistance** | **Elongation At Break** | **Layer Adhesion** | **Heat Resistance** | **Visual Quality** | **Ease Of Printing** |
| **ABS** | Medium | Medium | Medium | Medium | High | Medium | Medium |
| **PLA** | High | Low | Medium | High | Low | High | High |
| **Nylon** | Low | High | High | Low | Low | Medium | Medium |

PLA and ABS both exhibit better mechanical properties but it is PLA that offers ease in printing. With lower printing temperature, PLA is better suited to fabricate parts with finer details. PLA fabricated part is lesser prone to warping. ABS, on the other hand, is preferred for the fabrication of parts where strength, machinability along with thermal stability are required. PLA and ABS materials are available in typically the same cost and are listed among the common desktop FDM fabricated polymers (Tiwary et al., 2015). They are used for fabrication in blended forms also (added with additives to enhance the mechanical properties or with carbon fibers to make them stiffer).

Fabricating the products in a way similar to the printing media on the paper, FDM has gathered the attention of people from manufacturing industries and academia since long. Research has been carried out on the effect of processing parameters during fabrication on the product's tribological characteristics. Effect of governing process parameters like infill, build orientation, raster angle, layer height, and several contours have been studied on the surface characteristics, where it was found that tribological and surface characteristics were largely affected by the build orientation,raster angle, layer height and several contours (Mohamed et al., 2018 & Kumar et al., 2021). The study has also been conducted employing a genetic algorithm to get improved surface quality on FDM fabricated parts, where tests were carried out to find the optimal print orientation. Print orientation for this study was set as a factor affecting build-time, product cost, and product quality (Byun et al., 2006). The study shows that the nozzle-temperature and print orientation significantly responsible for crystallinity and affect material properties of heat resistant materials (Shouling et al., 2019). The investigation has been made by infusing bio-carbon in varying quantities to PLA to measure the frictional characteristics of fabricated parts (Ertane et al., 2018). In another study on wear using PoD, it was revealed that frictional force and wear rate was affected by built-orientation (Gurrala et al., 2017 & Srinivasan et al., 2020). A similar study on wear using PoD for parts made of a biomaterial used for hip replacement has also been conducted (Hussein et al., 2015 & Baykal et al., 2014). Interesting research, where artificial neural network (ANN) technique and quantum behaved particle swarm optimization (QPSO) were applied on process parameters to obtained optimal compressive stress, was conducted and found the results from the two in a good agreement (Sood et al., 2012). The influence of raster width, build orientation, and layer height on the impact and compressive strengths of polycarbonate have been investigated using the ANN technique (Darbar et al., 2017 & Omar et al., 2017). Experiments were conducted in studying the effect of variables like dimensional accuracy, time for the process, and energy demand during the process by 3D printer. Process parameters were chosen to be layer height, filling-pattern, build-orientation, printing plane, and part state during fabrication on build-platform. Taguchi optimization showed that the printing plane needed to be controlled for reducing the energy demand and the time taken for the process (Camposeco, 2020 & Vishal et al., 2020). Studies were made on optimizing the strength of FDM fabricated parts using Taguchi methodology (uz Zaman et al., 2019). From the literature, it is very clear that the properties of the printed part depend on the input parameters selected while fabricating the part. Hence, to enhance the properties of the (Gurrala et al., 2017 & Srinivasan et al., 2020). A similar study on wear using PoD for parts made of a biomaterial used for hip replacement has also been conducted (Hussein et al., 2015 & Baykal et al., 2014). Interesting research, where artificial neural network (ANN) technique and quantum behaved particle swarm optimization (QPSO) were applied on process parameters to obtained optimal compressive stress, was conducted and found the results from the two in a good agreement (Sood et al., 2012). The influence of raster width, build orientation, and layer height on the impact and compressive strengths of polycarbonate have been investigated using the ANN technique (Darbar et al., 2017 & Omar et al., 2017). Experiments were conducted in studying the effect of variables like dimensional accuracy, time for the process, and energy demand during the process by 3D printer. Process parameters were chosen to be layer height, filling-pattern, build-orientation, printing plane, and part state during fabrication on build-platform. Taguchi optimization showed that the printing plane needed to be controlled for reducing the energy demand and the time taken for the process (Camposeco, 2020 & Vishal et al., 2020). Studies were made on optimizing the strength of FDM fabricated parts using Taguchi methodology (uz Zaman et al., 2019). From the literature, it is very clear that the properties of the printed part depend on the input parameters selected while fabricating the part. Hence, to enhance the properties of the materials it is essential to identify the test the fabricated material and identify the conditions at which the properties are optimal. For the 3d printed materials, a lot of work has been reported regarding the measurement of different mechanical properties like tensile strength, compressive strength, impact etc. However, very few work have been reported regarding the measurement of wear rate.

In the present work, 3D printer parts have been fabricated at different combinations of input parameters using Flashforge Dreamer NX (Single extruder) 3D printer. These fabricated specimens have been examined to test the wear properties using a pin on disc wear testing machine. The obtained input and output have been used to generate an RSM based mathematical model. The model has been tested and a suitable range of input parameters has been identified by drawing the contour plots. The obtained range of input parameters has been verified by performing more experiments.

## EXPERIMENTATION

For fabricating the specimens, experiments have been performed on a Flashforge Dreamer NX (Single extruder) 3D printer as shown in Figure 1. The dimensions of the specimen have been taken as per the ASTM G 99 standard. The process parameters considered are layer thickness, print speed, and infill density. The fabricated specimens have been evaluated for the wear properties using a pin on disc wear testing machine. The process parameters and levels considered for experimentation have been shown in Table 2.

**Figure 1.** Flashforge Dreamer NX (Single extruder) 3D printer

| Process Parameter | Level 1 | Level 2 | Level 3 |
|---|---|---|---|
| Layer Thickness (A) | 0.20 | 0.25 | 0.30 |
| Print Speed (B) | 50 | 100 | 120 |
| Infill Density (C) | 70 | 80 | 90 |

Based on the Box Behnken design of experiments the full factorial design of 27 experiments has been reduced to 15 experiments. The design of the experiment has been shown in Table 3. From Table 2 it is very clear that there is a huge difference in the variables of the process parameters. Hence, the process parameters need to be converted in the coded form so that the response surface methodology can be implemented properly. The conversion of the process parameters have been done using the following equation:

$$A_{coded} = \frac{A-0.25}{0.05}; B_{coded} = \frac{B-100}{50}; C_{coded} = \frac{C-80}{10} \tag{1}$$

By performing these 15 sets of experiments 15 specimens have been fabricated. Some of the fabricated specimens have been shown in Figure 2. The wear rate of the specimens has been tested one after the other using the pin on disc wear testing machine as shown in Figure 3. The recorded wear rate has been shown in Table 3. Table 4 shows the parameters of the pin on disc machine that have been keen constant while performing the testing.

**Table 3.** Design of Experiment and obtained wear rate

| Experiment No. | A | A(coded) | B | B(coded) | C | C(coded) | Wear Rate (*10-2) |
|---|---|---|---|---|---|---|---|
| 1 | 0.30 | 1 | 100 | 0 | 70 | -1 | 1.4638 |
| 2 | 0.25 | 0 | 50 | -1 | 70 | -1 | 1.2732 |
| 3 | 0.25 | 0 | 150 | 1 | 70 | -1 | 1.5786 |
| 4 | 0.25 | 0 | 100 | 0 | 80 | 0 | 1.6829 |
| 5 | 0.20 | -1 | 100 | 0 | 70 | -1 | 1.6528 |
| 6 | 0.20 | -1 | 150 | 1 | 80 | 0 | 1.7977 |
| 7 | 0.30 | 1 | 50 | -1 | 80 | 0 | 1.5681 |
| 8 | 0.25 | 0 | 100 | 0 | 80 | 0 | 1.6829 |
| 9 | 0.20 | -1 | 50 | -1 | 80 | 0 | 1.7571 |
| 10 | 0.25 | 0 | 100 | 0 | 80 | 0 | 1.6829 |
| 11 | 0.30 | 1 | 100 | 0 | 90 | 1 | 1.7130 |
| 12 | 0.25 | 0 | 150 | 1 | 90 | 1 | 1.2278 |
| 13 | 0.25 | 0 | 50 | -1 | 90 | 1 | 1.7872 |
| 14 | 0.30 | 1 | 150 | 1 | 80 | 0 | 1.6087 |
| 15 | 0.20 | -1 | 100 | 0 | 90 | 1 | 1.9020 |

**Table 4.** Pin-on-disc machine parameters

| | |
|---|---|
| Time (minutes) | 50 (Minutes) |
| RPM (Revolution per minute) | 150 |
| Track Diameter (mm) | 70 |
| Load (Kg) | 5 |
| Sliding Distance (m) | 1648.5 |

All these parameters were kept constant throughout the testing.

**Figure 2.** Fabricated specimen

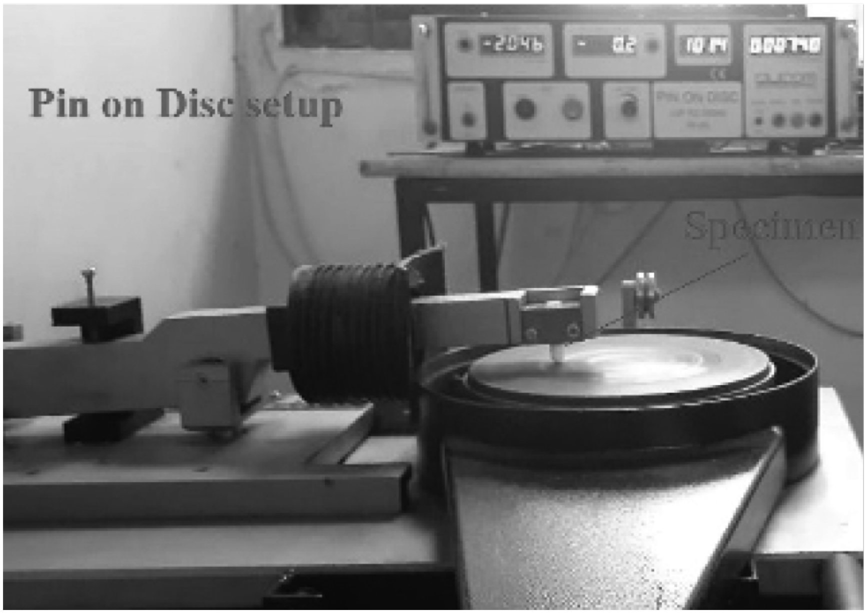


**Figure 3.** Pin on disc setup

## MODELING USING RESPONSE SURFACE METHODOLOGY

The data shown in Table 3 have been used to develop the mathematical model based on response surface methodology (Shrivastava et al., 2018 & Ferreira et al., 2007) using MINITAB 19. While modeling the confidence level for intervals has been taken as 95%. The generated model has been shown in equation 2. To analyze the model, an ANOVA table has also been drawn as shown in Table 5. Which shows that the model is significant with p-value less than 0.05, also the R square value of the generated model is 94.17%, and the input parameter A and C have higher significance as compared to B. Moreover, to identify the accuracy of the developed model, predicted values for each combination of input parameters have been calculated as shown in Table 6. Thereafter, a comparison plot has been drawn to identify the percentage error between the experimental and predicted values as shown in Figure 4. From the plot, it has been found that the average percentage error between the experimental and predicted values is 2.229%.

**Table 5.** Analysis of Variances

| Source | DF | Adi SS | F-Value | P-Value |
|---|---|---|---|---|
| Model | 9 | 0.453970 | 8.98 | 0.013 |
| Linear | 3 | 0.129889 | 7.71 | 0.025 |
| A | 1 | 0.071442 | 12.72 | 0.016 |
| B | 1 | 0.003732 | 0.66 | 0.452 |
| C | 1 | 0.054714 | 9.74 | 0.026 |
| Square | 3 | 0.137111 | 8.14 | 0.023 |
| A*A | 1 | 0.043147 | 7.68 | 0.039 |
| B*B | 1 | 0.043147 | 7.68 | 0.039 |
| C*C | 1 | 0.043147 | 7.68 | 0.039 |
| 2-Way Interaction | 3 | 0.186970 | 11.09 | 0.012 |
| A*B | 1 | 0.000000 | 0.00 | 1.000 |
| A*C | 1 | 0.000000 | 0.00 | 1.000 |
| B*C | 1 | 0.186970 | 33.28 | 0.002 |
| Error | 5 | 0.028090 | | |
| Lack-of-Fit | 3 | 0.028090 | * | * |
| Pure Error | 2 | 0.000000 | | |
| Total | 14 | 0.482059 | | |

$$\begin{aligned} Wear\ Rate = {} & 1.6829\ -0.0945A\ -0.0216B\ +0.0827C\ +0.1081A*A \\ & -0.1081B*B-0.1081C*C-0.2162B*C \end{aligned} \tag{2}$$

**Table 6.** Predicted values and percentage error

| Exp. No. | A | B | C | Wear Rate(*10-2) | Predicated | Error |
|---|---|---|---|---|---|---|
| 1 | 0.3 | 100 | 70 | 1.4638 | 1.5057 | 2.862413 |
| 2 | 0.25 | 50 | 70 | 1.2732 | 1.1894 | 6.581841 |
| 3 | 0.25 | 150 | 70 | 1.5786 | 1.5786 | 0 |
| 4 | 0.25 | 100 | 80 | 1.6829 | 1.6829 | 0 |
| 5 | 0.2 | 100 | 70 | 1.6528 | 1.6847 | 2.535092 |
| 6 | 0.2 | 150 | 80 | 1.7977 | 1.7558 | 2.330756 |
| 7 | 0.3 | 50 | 80 | 1.5681 | 1.61 | 2.672023 |
| 8 | 0.25 | 100 | 80 | 1.6829 | 1.6829 | 0 |
| 9 | 0.2 | 50 | 80 | 1.7571 | 1.799 | 2.384611 |
| 10 | 0.25 | 100 | 80 | 1.6829 | 1.6829 | 0 |
| 11 | 0.3 | 100 | 90 | 1.713 | 1.6711 | 2.446001 |
| 12 | 0.25 | 150 | 90 | 1.2278 | 1.3116 | 6.825216 |
| 13 | 0.25 | 50 | 90 | 1.7872 | 1.7872 | 0 |
| 14 | 0.3 | 150 | 80 | 1.6087 | 1.5668 | 2.604588 |
| 15 | 0.2 | 100 | 90 | 1.902 | 1.8606 | 2.202944 |
| | | | | | | 2.229699 |
| | Average Percentage Deviation | | | | | 2.229699 |

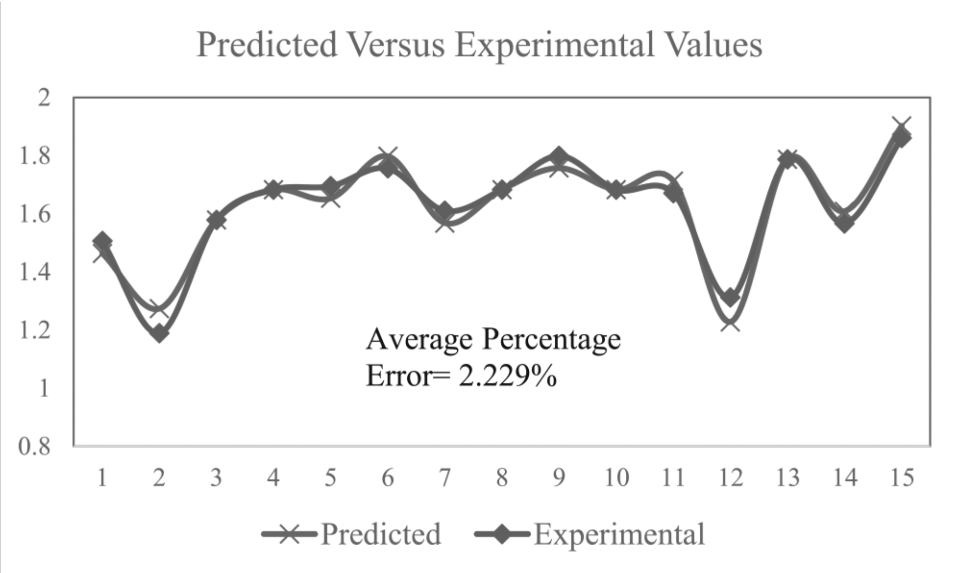


**Figure 4.** Experimental Versus Predicted Values

## RESULTS AND DISCUSSION

In order to identify the suitable combination of input parameters for fabricating the specimen which can have a minimum wear rate, contour plots have been drawn as shown in Figure 5-7. In these figures, different color regions have been shown separated by contour lines. The region with blue and violet color reflects the maximum value of wear. Similarly, the region having red color resembles the minimum wear. Likewise, the yellow color resembles intermediate values of wear.From the figures, it has been perceived that if a suitable combination of input parameters are considered, the resulting wear rate can be minimized. For selecting the input parameters. The contour plots have been analyzed thoroughly. The plot showing variation between 'A', 'C' and wear rate resembles that, if the value of 'A' is kept between (0.24 to 0.28) and coded value of 'C' is kept between (70 to 73 or 87 to 90), then the wear rate will be intermediate. Similarly, for plots showing variation between 'A', 'B', and wear rate. 'A' should be kept between (0.23 to 0.28) and 'B' should be kept between (140 to 150) for intermediate wear rate. In case of variation between 'B', 'C', and wear rate. The values for 'B' can be between (140 to 150), 'C' between (85 to 90). These ranges of input parameters have been merged together to obtain a single range as shown in Table 7.

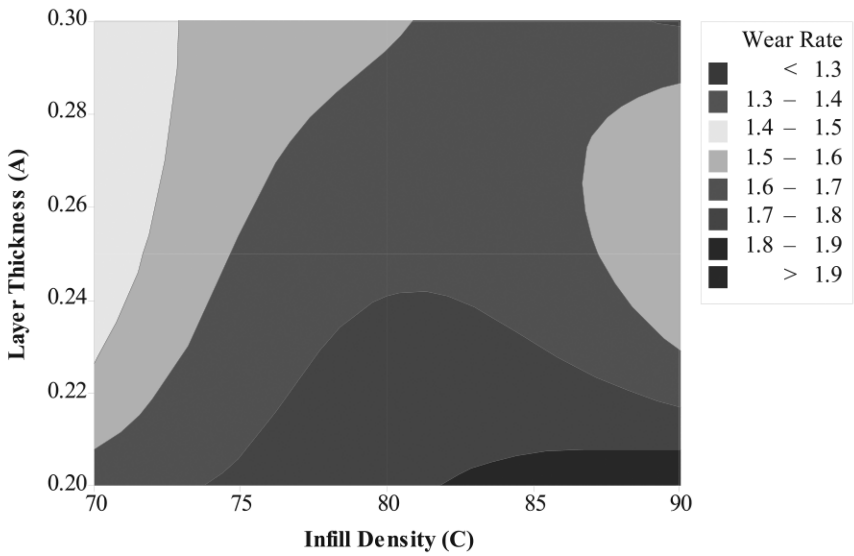


**Figure 5.** Contour plot for wear rate showing variation between layer thickness and Infill density

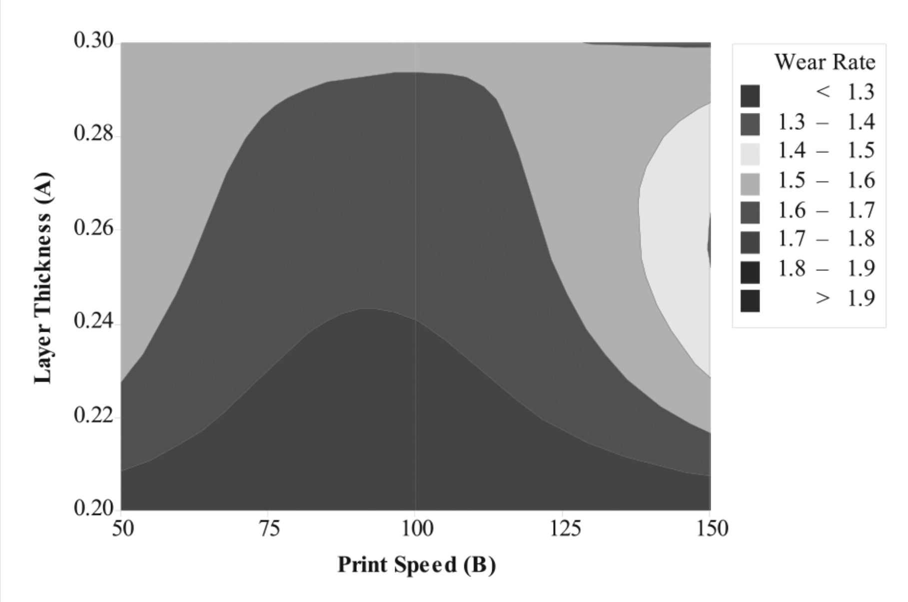


**Figure 6.** Contour plot for wear rate showing variation between layer thickness and print speed

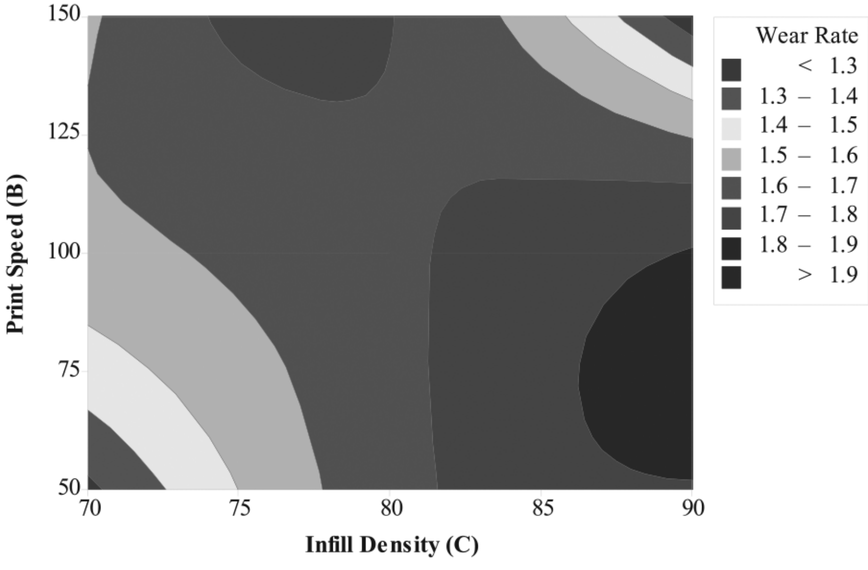


**Figure 7.** Contour plot for wear rate showing variation between print speed and Infill density

The suitable range obtained in Table 7 indicates the most suitable range of input parameters for fabricating the specimens at given condition so that the wear rate will be minimum. In order to verify the obtained range, more fabrication and testing of specimens have been performed. The details of the process parameters and testing results have been shown in Table 8.

**Table 8.** Validation Experiments

| Verification Experiment No. | A (mm) | B (mm/sec) | C (%) | Wear rate (*10^-2) |
|---|---|---|---|---|
| **1.** | **0.25** | **150** | **90** | **1.2871** |
| **2.** | **0.27** | **150** | **90** | **1.2113** |
| **3.** | **0.25** | **140** | **90** | **1.3065** |

From the results, it has been perceived that the obtained range of input parameters is significant as the calculated wear rate is low. Hence, for the given conditions, the obtained range of input parameters can be considered for fabricating the specimens resulting in an acceptable wear rate.

## CONCLUSIONS

The present work is focused on the identification of suitable process parameters of a Flashforge Dreamer NX (Single extruder) 3D printer for the fabrication of specimens that may result in a low wear rate. For this, specimens have been fabricated at different combinations of process parameters, the fabricated specimens have been tested using a Pin-on-disc machine wear testing machine. The obtained results have been used to generate the mathematical model using the RSM. The key findings of the present work are:

1. The developed model is significant as the R sq. value is 94.17%, the P-value of the model is less than 0.05.
2. The variation between the experimental and predicted value is 2.229%, which indicates that the model can predict the appropriate values.
3. From the ANOVA table it has been perceived that in the comparison between the three input parameters, layer thickness and Infill density are more significant than the print speed for given conditions.
4. From the results it has been found that if parameter A is selected in between the range of 0.24-0.28, B is selected between 140-150, and C must be kept between 87-90 then the obtained specimen will have a lower wear rate.

## REFERENCES

**Calignano,. F, Manfredi, D., Ambrosio, E.P., Biamino, S., Lombardi, M., Atzeni, E., Salmi, A.,**

**Minetola, P., Iuliano, L. & Fino, P. 2017.** Overview on additive manufacturing technologies. Proceedings of the IEEE 105 (4): 593-612.

**Negi, S., Dhiman, S. & Sharma, R.K. 2014.** Basics and applications of rapid prototyping medical models. Rapid Prototyping Journal

**Srivastava, M. & Rathee, S. 2018.** Optimisation of FDM process parameters by Taguchi method for imparting customised properties to components. Virtual and Physical Prototyping. 13 (3):203-210..

**Yadav, A., Srivastav, A., Singh, A., Mushtaque, M.D., Khan, S.A., Kumar, H. & Arora, P.K. 2021.** Investigation on the materials used in additive manufacturing: A study. Materials Today: Proceedings. ISSN 2214-7853, https://doi.org/10.1016/j.matpr.2020.10.975.

**Mercado, F. & Rojas, A.A. 2020.** Additive manufacturing methods: techniques, materials, and closed-loop control applications. The International Journal of Advanced Manufacturing Technogy lo.109. 10.1007/s00170-020-05663-6.

**Gao, W., Zhang, Y., Ramanujan, D., Ramani, K., Chen, Y., Williams, C.B., Wang, C.C., Shin, Y.C., Zhang, S. & Zavattieri, P.D. 2015.** The status, challenges, and future of additive manufacturing in engineering. Computer-Aided Design. 69: 65-89.

**Mellor, S., Hao, L. & Zhang, D. 2014.** Additive manufacturing: A framework for implementation. International journal of production economics. 149: 194-201.

**Selimis, A. & Farsari, M. 2017.** 3.8 Laser-Based 3D Printing and Surface Texturing, Editor(s): MSJ Hashmi, Comprehensive Materials Finishing, Elsevier, Pages 111-136, ISBN 9780128032497.

**ASTM International. 2012.** ASTM Committee F42 on Additive Manufacturing Technologies. Subcommittee F42. 91 on Terminology. Standard Terminology for Additive Manufacturing Technologies.

**ISO / ASTM52900-15. 2015.** Standard Terminology for Additive Manufacturing – General Principles – Terminology, ASTM International, West Conshohocken, PA, www.astm.org

**Gibson, I., Rosen, D., Stucker, B. & Khorasani, M. 2014.** Additive manufacturing technologies. 17. Springer.

**Novakova-Marcincinova, L. 2012.** Application of fused deposition modeling technology in 3D printing rapid prototyping area. Manuf and Ind Eng. 11 (4):35-37.

**Sahmani, S., Khandan, A., Esmaeili, S., Saber-Samandari, S., Nejad, M.G. & Aghdam, M. 2020.** Calcium phosphate-PLA scaffolds fabricated by fused deposition modeling technique for bone tissue applications: fabrication, characterization and simulation. Ceramics International. 46 (2):2447-2456.

**Agnieszka, H., Iga, C., Paulina, K., Kamil, S., Marcin, Ł., Marta, P., Justyna, K. & Helena, J. 2020.** A comprehensive evaluation of flexible FDM/FFF 3D printing filament as a potential material in medical application, European Polymer Journal, Volume 138, 109958, ISSN 0014-3057.

**Sylvain, C., Noelia, M., Sanchez-Ballester, Yanis A.G., Bernard, B. & Ian, S. 2021.** Fused Deposition Modeling (FDM), the new asset for the production of tailored medicines, Journal of Controlled Release, Volume 330, Pages 821-841, ISSN 0168-3659.

**Alhijjaj, M., Belton, P. & Qi, S. 2016.** An investigation into the use of polymer blends to improve the printability of and regulate drug release from pharmaceutical solid dispersions prepared via fused deposition modeling (FDM) 3D printing. European Journal of Pharmaceutics and Biopharmaceutics. 108:111–25.

**Yang, Y., Wang, H., Li, H., Ou, Z. & Yang, G. 2018.** 3D printed tablets with internal scaffold structure using ethyl cellulose to achieve sustained ibuprofen release. Eur J Pharm Sci. 115:11–8.

**Kejing, S., Jonathan, P.S., Mohammed, M. & Ali, N. 2021.** Role of release modifiers to modulate drug release from fused deposition modelling (FDM) 3D printed tablets, International Journal of Pharmaceutics, Volume 597, 120315, ISSN 0378-5173.

**Srinivasan, R., Aravindkumar, N., Aravind, K.S., Aadhishwaran, S. & John, G. 2020.** Influence of fused deposition modelling process parameters on wear strength of carbon fibre PLA, Materials Today: Proceedings, Volume 27, Part 2, Pages 1794-1800, ISSN 2214-7853.

**Hussein, M.A., Mohammed, A.S. & Al-Aqeeli, N. 2015.** Wear characteristics of metallic biomaterials: a review. Materials 8 (5):2749-2768.§

**Baykal, D., Siskey, R.S., Haider, H., Saikko, V., Ahlroos, T. & Kurtz, S.M. 2014.** Advances in tribological testing of artificial joint biomaterials using multidirectional pin-on-disk testers, Journal of the Mechanical Behavior of Biomedical Materials. 31: 117-134, ISSN 1751-6161.

**Sood, A.K., Ohdar, R.K. & Mahapatra, S.S. 2012.** Experimental investigation and empirical modelling of FDM process for compressive strength improvement. Journal of Advanced Research. 3(1):81-90.

**Darbar, R. & Patel, P.M. 2017.** Optimization of fused deposition modeling process parameter for better mechanical strength and surface roughness. International Journal of Mechanical Engineering. 6:7-18.

**Omar, A.M., Syed, H.M., Jahar, L.B. & Anthony, E.S. 2017.** Investigation on the tribological behavior and wear mechanism of parts processed by fused deposition additive manufacturing process. Journal of Manufacturing Processes. 29:149-159, ISSN 1526-6125.

**Camposeco-Negrete, C. 2020.** Optimization of FDM parameters for improving part quality, productivity and sustainability of the process using Taguchi methodology and desirability approach. Progress in Additive Manufacturing. 5 (1):59-65.

**Vishal, W., Darshit, J., Akshata, J. & Rakesh, C. 2020.** Experimental investigation of FDM process parameters using Taguchi analysis, Materials Today: Proceedings. 27(3): 2117-2120, ISSN 2214-7853.

**uz Zaman, U.K., Boesch, E., Siadat, A., Rivette, M. & Baqai, A.A. 2019.** Impact of fused deposition modeling (FDM) process parameters on strength of built parts using Taguchi's design of experiments. The international journal of Advanced Manufacturing technology. 101(5):1215-1226.

**Shrivastava, Y., Singh, B. 2018.** Estimation of stable cutting zone in turning based on empirical mode decomposition and statistical approach. Journal of the Brazilian Society of Mechanical Sciences and Engineering. 40 (2):77.

**Ferreira, S.C., Bruns, R., Ferreira, H., Matos, G., David, J., Brandao, G., da Silva, E.P., Portugal, L., Dos Reis, P. & Souza, A. 2007.** Box-Behnken design: An alternative for the optimization of analytical methods. Analytica chimica acta. 597 (2):179-186.